

# CH<sub>3</sub>SH conversion in a tubular flow reactor. Experiments and kinetic modelling

M.U. Alzueta,\*R. Pernía, M. Abián, Á. Millera, R. Bilbao

Aragón Institute of Engineering Research (I3A), Department of Chemical and Environmental Engineering, University of Zaragoza, C/Mariano Esquillor s/n, Zaragoza 50018, Spain.

e-mail: uxue@unizar.es (corresponding author: M.U. Alzueta, Spain)

## Abstract

The use of non-conventional fuel sources, such as shale gas, brings new research requisites for its proper use in an environmental friendly manner. In this context, shale gas may include different sulphur containing compounds, such as methanethiol, that is also formed as intermediate during sulphur containing residues processing. The present work includes an experimental and kinetic modelling study of the oxidation of methanethiol, CH<sub>3</sub>SH, in a quartz flow tubular reactor at atmospheric pressure and in the 300-1400 K temperature range. The influence of the temperature, the O<sub>2</sub> concentration and the presence of H<sub>2</sub>O on the conversion regime of CH<sub>3</sub>SH and the formation of different compounds has been analysed. The experimental results have been interpreted in terms of a detailed gas-phase mechanism compiled in the present work, and the elementary steps involved in the conversion of CH<sub>3</sub>SH have been identified.

In general, oxidation of CH<sub>3</sub>SH is favoured by both oxygen level and temperature, while the presence of H<sub>2</sub>O does not modify the CH<sub>3</sub>SH conversion profile. The main sulphur containing products are SO<sub>2</sub>, H<sub>2</sub>S and CS<sub>2</sub>, pointing to a significant role of other products, apart from SO<sub>2</sub>, for the control of pollutant emissions.

**Keywords:** CH<sub>3</sub>SH, methyl mercaptan, methanethiol, oxidation, sour gas, shale gas, PFR, kinetic modelling

## INTRODUCTION

The use of non-conventional fuel sources, such as shale gas, refinery gas, or biogas obtained from anaerobic digestion, brings new research requisites for its proper use in an environmental friendly manner. In this context, these gases, apart from  $\text{CH}_4$  and  $\text{CO}_2$ , may include different sulphur containing compounds, such as hydrogen sulphide and mercaptans as methanethiol, that is also formed as intermediate during sulphur containing residues processing. The presence of sulphur in sour gases makes more difficult its application, mainly because of environmental issues. While the traditional way to use these fuels is based on their exhaustive cleaning [e.g. 1], the present strategies include the direct use of sour gases in combustion together with the improvement of technologies and combustion processes, along with the later solution of environmental problems. This is what has been named as a “double revolution” [2].

Methanethiol,  $\text{CH}_3\text{SH}$ , also known as methyl mercaptan, is a sulphur organic compound that can be present in a number of fuel gases, such as natural gas, sour gas, shale gas, biogas or refinery gas [3]. Formation of mercaptans (mainly  $\text{CH}_3\text{SH}$ ), together with  $\text{COS}$  and  $\text{CS}_2$  also occurs in the Claus process through the interaction of  $\text{CO}_2$ , hydrocarbon radicals and sulphur species [4], reducing thus the sulphur recovery efficiency. Shale gas has been reported to contain typically a total sulphur content of up to 1 %, including sulphur in pyritic form, sulfates and organics [5], with concentrations of mercaptans ( $\text{CH}_3\text{SH}$ ) of up to 0.5 % [6].  $\text{CH}_3\text{SH}$  can also be formed as an intermediate compound in the destruction of mustard gas,  $\text{ClCH}_2\text{-CH}_2\text{-S-CH}_2\text{-CH}_2\text{Cl}$ , through incineration mainly chosen as a high effectiveness destruction method, even though there is still significant concern over the potential formation of toxic emissions [7, 8]. Under oxidation conditions, conversion of  $\text{CH}_3\text{SH}$  may lead preferably to  $\text{SO}_2$ , but also to  $\text{H}_2\text{S}$  or other carbon-sulphur compounds such as  $\text{COS}$  or even  $\text{CS}_2$ .

While the conversion of  $\text{COS}$  and  $\text{CS}_2$  have been considered in the past [e.g. 9-11], to our knowledge, no investigation of the oxidation of  $\text{CH}_3\text{SH}$  has been carried out under combustion conditions. However, significant efforts have been drawn to evaluate the oxidation of  $\text{CH}_3\text{SH}$  in the atmosphere, because of its probable and significant role in the atmospheric sulphur cycle (e.g. [12-14]). Actually, methanethiol has been reported to represent around a 10 % of the global flux of sulphur compounds in the atmosphere [15].

In this context, the present study aims to carry out a combined experimental and kinetic modelling study of the conversion of  $\text{CH}_3\text{SH}$  under combustion conditions. The impact of temperature and stoichiometry, ranging from almost pyrolysis to very oxidizing conditions, on the process is evaluated in a tubular flow reactor at atmospheric pressure and in the 300-1400 K temperature range. Experimental results are discussed in terms of a detailed kinetic mechanism. The present study is of interest in its own right, and may serve as a base case to consider the behavior of non-aromatic organic sulphur in combustion systems.

## EXPERIMENTAL METHODOLOGY

Most of the experiments have been carried out in a quartz tubular flow reactor at atmospheric pressure. Only a brief experimental setup (setup 1) description is given here and a more detailed description can be found elsewhere [16]. The reactor has an isothermal reaction zone of 20 cm in length and 0.87 cm of internal diameter. Total flow rate in all experiments was 1 L (STP)/min, resulting in a gas residence time as a function of temperature of  $194.6/T(\text{K})$ , in seconds. The reactor is placed in a three-zone electrically heated oven, ensuring a uniform temperature profile ( $\pm 5$  K) along the reaction zone. Experiments are carried out under highly diluted conditions using nitrogen as bath gas. Gases from cylinders are led to the reactor in up to four separate streams, following the procedure of Alzueta et al. [17], and are heated separately and mixed in cross flow at the reactor inlet. At the outlet of the reaction zone, the product gas is quenched by means of external cooling air. The exhaust gases go

through a condenser and a filter, removing any possible residual solid and moisture, and subsequently conducted to the analysis system, which includes a UV continuous analyser for SO<sub>2</sub>, an IR continuous analyser for CO and CO<sub>2</sub> and a gas micro-chromatograph for CH<sub>3</sub>SH, H<sub>2</sub>S, COS, CS<sub>2</sub>, CH<sub>4</sub>, CO, CO<sub>2</sub>, O<sub>2</sub> and H<sub>2</sub> quantification. The uncertainty of the measurements is estimated within 5 %.

Additionally, with the purpose of evaluating a strange behavior found in CO formation that will be described later in detail, one experiment has been performed in a different installation (setup 2) that is described in a previous work by our group [18].

## KINETIC MODEL

The experimental results have been interpreted in terms of an updated kinetic model. The mechanism used is based on the mechanism by Alzueta et al. [19] developed to analyse the impact of the presence of SO<sub>2</sub> on fuel conversion, and includes the interaction of SO<sub>2</sub> with CO and small hydrocarbons by Glarborg et al. [20, 21]. This mechanism was later updated by Giménez-López et al. [22] to account for oxy-fuel combustion conditions. To the updated mechanism, we have added a CH<sub>3</sub>SH conversion subset, and related thermochemistry, taken mainly from the works of Zheng et al. [7, 23] and Van de Vijver et al. [24], who studied respectively the oxidation of diethyl sulphide and the pyrolysis of alkyl sulphides. The work of Van de Vijver et al. [24] is, in turn, largely based on previous works by the group [25-29]. This reaction subset has also been largely used in the recent work of Gersen et al. [30], who studied the effect of H<sub>2</sub>S addition on methane ignition and oxidation at high pressure. Subsets for COS and CS<sub>2</sub> conversion were taken from previous works from the authors [31, 32] and the H<sub>2</sub>S conversion subset from a recent work by our group [33]. This H<sub>2</sub>S reaction subset is largely based on the works of Sendt et al. [34], Zhou et al. [35] and Song et al. [36]. The mechanism of Colom-Díaz et al. [33] included the isomerization of HSOO to HSO<sub>2</sub>, as a key fast step for H<sub>2</sub>S oxidation, together with new kinetic parameters for the  $\text{SH} + \text{H}_2\text{O}_2 \rightleftharpoons \text{H}_2\text{S} + \text{HO}_2$  reaction, which was found to have a significant impact on H<sub>2</sub>S conversion, and that is included in the present mechanism, since the formation of significant amounts of H<sub>2</sub>S from methanethiol can be expected.

The final reaction mechanism listing is included as supplementary material. As for thermochemical data, same sources as for the corresponding reactions were used. Calculations were carried out using the PFR model of the Chemkin Pro suite [37].

## RESULTS AND DISCUSSION

The study of CH<sub>3</sub>SH oxidation in a tubular flow reactor at atmospheric pressure has been carried out from almost pyrolysis to fuel-lean conditions, in the temperature range of 300-1400 K. The experimental conditions studied are listed in Table 1. The influence of the amount of oxygen available on the process was studied for different values of  $\lambda$ , defined as O<sub>2</sub>(real)/O<sub>2</sub>(stoichiometric). For an inlet total flow rate of 1 L (STP)/min, the gas residence time in the reactor varies in the 0.14-0.24 seconds range depending on temperature, according to 194.6/T(K), with the exception of experiment 8, for which the residence time is 414/T(K) seconds.

Table 1: Experimental conditions. Experiments 1 to 7 are performed at atmospheric pressure in setup 1 [16]. Experiment 8 is performed at 1.81 bar in setup 2 [18].

Set	CH <sub>3</sub> SH (ppm)	O <sub>2</sub> (ppm)	H <sub>2</sub> O (%)	$\lambda$	Setup
1	983	42	-	0.01	1
2	968	1211	-	0.42	1
2a	972	979	0.5	0.34	1
3	977	2269	-	0.77	1
4	952	2841	-	0.99	1
4a	1003	2953	0.5	0.98	1
4r	965	2841	-	0.98	1
5	965	4576	-	1.58	1
6	973	5878	-	2.01	1
7	973	14855	-	5.08	1
7a	1015	13370	0.5	4.39	1
8	987	3025	-	1.02	2

For the conditions listed in Table 1, the concentrations of CH<sub>3</sub>SH, SO<sub>2</sub>, H<sub>2</sub>S, O<sub>2</sub>, CO, CO<sub>2</sub>, H<sub>2</sub>, CH<sub>4</sub> and CS<sub>2</sub> obtained as a function of temperature are presented in Figure 1.

Figure 1 shows the experimental results for the quantified species during the conversion of CH<sub>3</sub>SH as a function of temperature and for the different stoichiometries studied ( $\lambda$  values ranging from almost pyrolysis conditions to very fuel-lean conditions), in the absence of water. Experimental sulphur and carbon mass balances close to 100±5 % in most cases, except for carbon at intermediate temperatures (823-923 K) where the balance goes down to 70-75 %. This is attributed to the fact that the sharpest conversion of CH<sub>3</sub>SH occurs in this temperature interval, with many intermediates in small concentrations that appear and are not quantified.

Methanethiol starts its conversion between 800 and 1000 K as a function of stoichiometry, with the onset conversion temperature shifted towards lower temperatures as the oxygen availability in the reaction environment is higher. Most of CH<sub>3</sub>SH conversion occurs in a narrow temperature range of about 50 K. The final products dominant in CH<sub>3</sub>SH conversion include H<sub>2</sub>, CO, CO<sub>2</sub>, and SO<sub>2</sub> as sulphur species. With the exception of CO and SO<sub>2</sub> (under fuel-rich conditions), which exhibit a maximum as a function of temperature, the rest of dominant final products increase with temperature under the conditions considered. It is worthwhile to mention that, for the highest temperatures (above 1000 K approximately) and the fuel leaner stoichiometries ( $\lambda=1.5$  and above), the sulphur present in CH<sub>3</sub>SH is fully converted to SO<sub>2</sub>. For  $\lambda<1$ , conversion of CH<sub>3</sub>SH also results in the formation

of intermediates, as  $\text{CH}_4$  and  $\text{H}_2\text{S}$ , which exhibit a maximum that is shifted to lower temperatures, as the stoichiometry becomes fuel leaner. It is noticeable that, under the fuel-rich conditions studied,  $\text{CH}_4$  and  $\text{H}_2\text{S}$  are still present even at the highest temperatures considered. It is also remarkable that  $\text{CS}_2$  is formed in all the experiments, appearing in significant concentrations under fuel-rich conditions, while  $\text{COS}$  ( $\text{O}=\text{C}=\text{S}$ ) was found in the range of few ppm, only under reducing conditions ( $\lambda < 0.7$ ) and at the highest temperature considered in the present study. This is in agreement with earlier studies [31], where the formation of  $\text{COS}$  has been reported to be formed in the oxidation of  $\text{CS}_2$ . Under reducing conditions, the formation of a yellow powder was observed at the outlet of the reactor, but its quantification was not possible, as also happened in previous works by our group [33]. The kinetic model used in the present work also predicts the formation of small amounts of  $\text{S}_2$  under reducing conditions.

The results shown in Figure 1 correspond to experiments performed in the absence of water vapour. In order to evaluate the impact of the presence of water, which has been reported to shift the conversion of  $\text{CO}$  in the presence of  $\text{SO}_2$  [20], experiments in the presence of water (0.5 %) have been performed, and the results obtained in both the absence and presence of water are shown in Figure 2. As an example, for fuel-rich conditions, Figure 2a shows that the results with and without water are very similar for all the species measured, despite the slight differences between the two experiments in relation to the initial concentrations of  $\text{CH}_3\text{SH}$  and  $\text{O}_2$  (968 and 972 ppm, and 1211 and 979 ppm, respectively), which result in a slightly different  $\lambda$  value (0.42 and 0.34 respectively), and the slightly different pressures (1 and 1.8 bar respectively). Similar findings were obtained for other stoichiometries (Figures 2b and 2c). From these results, and under the conditions considered in the present work, no impact of water presence on the conversion of  $\text{CH}_3\text{SH}$  can be drawn.

In order to further explore the performance of the experiments, Figure 3 shows an example of the repeatability of experiments for the case of  $\lambda=1$ . The results show a good repeatability of all the different species concentrations measured, and the slight differences observed can be attributed to the non-exactly equal initial conditions of experiments 4 and 4r in Table 1.

As has been mentioned earlier, we have used a chemical detailed mechanism to interpret the experimental data of methanethiol conversion under the studied conditions in the present work. Figure 4 shows, as an example, the comparison between the experimental results and calculations for three selected stoichiometries (fuel-rich:  $\lambda=0.77$ , stoichiometric:  $\lambda=0.99$ , and fuel-lean:  $\lambda=5.08$ , sets 3, 4 and 7 in Table 1). Symbols represent experimental data and lines indicate model predictions using the mechanism compiled in this work. As seen, the model reproduces fairly well both the tendencies and the concentrations of the different compounds, through all the temperature range considered and for the different stoichiometries, with the exception of  $\text{CO}$  at temperatures below approximately 1200 K. A similar agreement is obtained for the rest of stoichiometries studies, not shown.

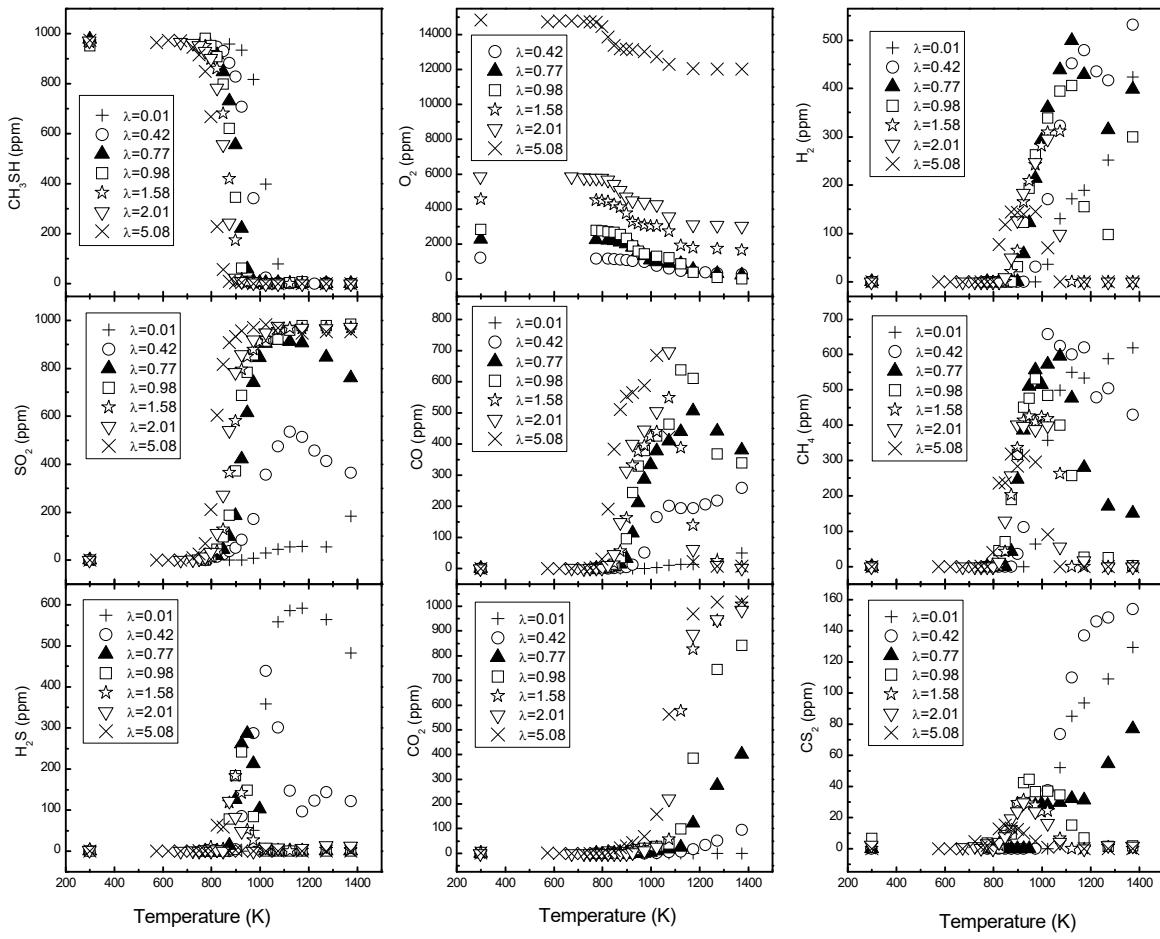


Figure 1. Experimental concentrations of  $\text{CH}_3\text{SH}$ ,  $\text{SO}_2$ ,  $\text{H}_2\text{S}$ ,  $\text{O}_2$ ,  $\text{CO}$ ,  $\text{CO}_2$ ,  $\text{H}_2$ ,  $\text{CH}_4$  and  $\text{CS}_2$  as a function of temperature for different stoichiometries. Results correspond to sets 1 to 7 in Table 1.

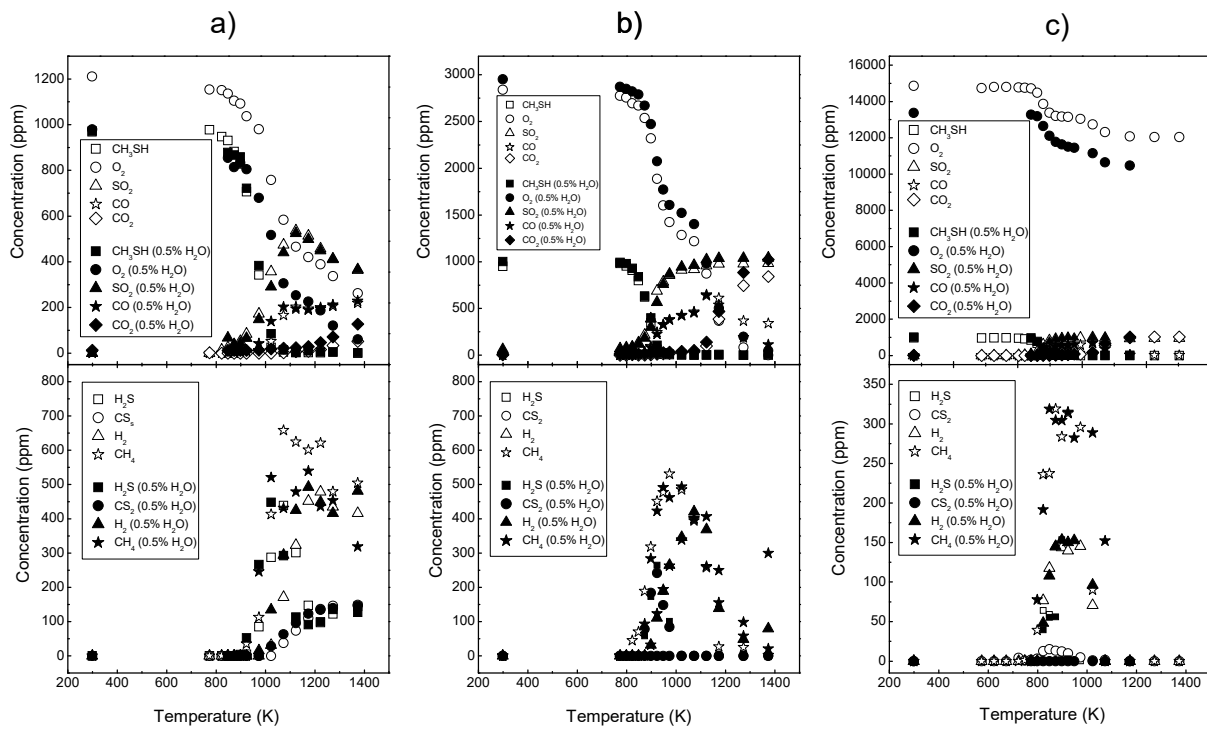


Figure 2. Experimental concentrations of CH<sub>3</sub>SH, SO<sub>2</sub>, H<sub>2</sub>S, O<sub>2</sub>, CO, CO<sub>2</sub>, H<sub>2</sub>, CH<sub>4</sub> and CS<sub>2</sub> as a function of temperature both in the absence and presence of water (0.5 %) and for rich, stoichiometric and fuel-lean conditions. Results of a) graphs correspond to sets 2 and 2a (fuel-rich conditions); results of b) graphs correspond to sets 4 and 4a (stoichiometric conditions); and results of c) graphs correspond to sets 7 and 7a (fuel-lean conditions) in Table 1.

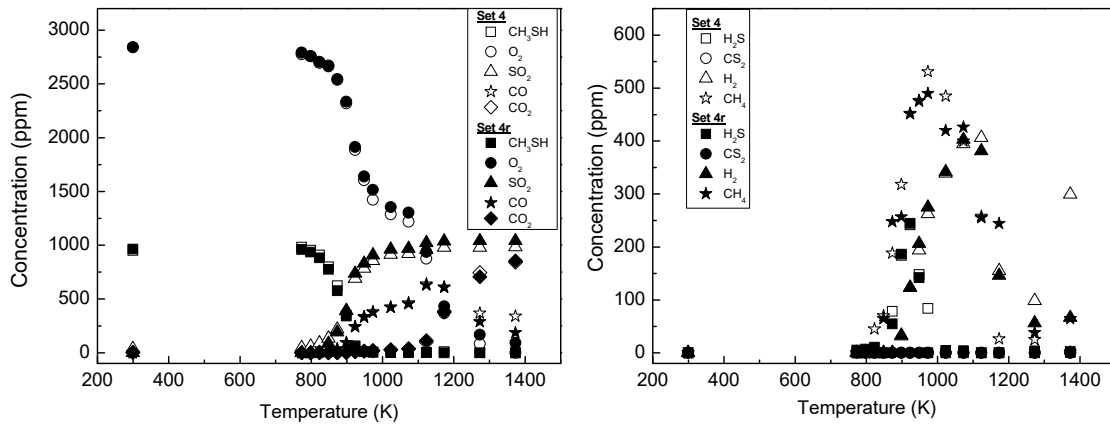


Figure 3. Example of the repeatability of experiments. Experimental data correspond to experiments 4 and 4r in Table 1.

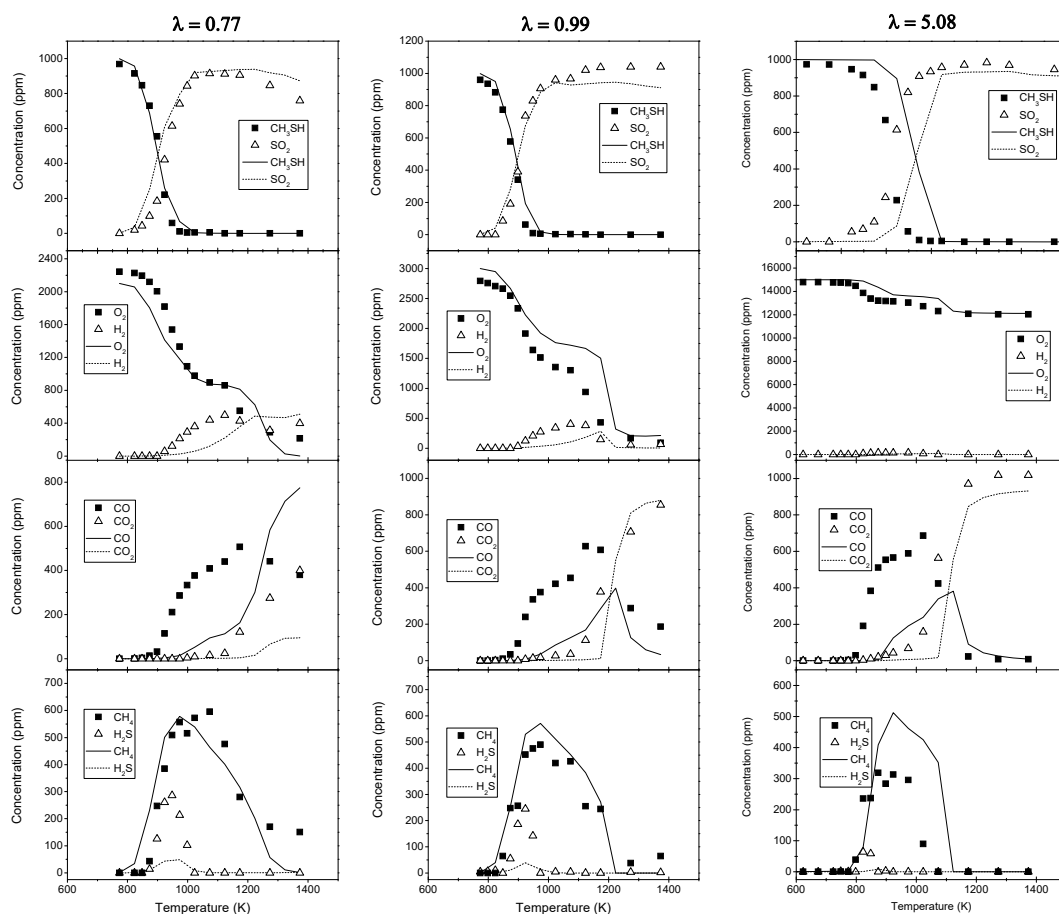


Figure 4. Comparison between simulations and experimental results for  $\lambda=0.77$  (set 3 in Table 1),  $\lambda=0.99$  (set 4 in Table 1), and  $\lambda=5.08$  (set 7 in Table 1).

While the experimental CO concentration exhibits an early formation coinciding with  $\text{CH}_3\text{SH}$  diminution, the model does not capture this behaviour. It has to be mentioned that the concentration of CO in the experiments was measured simultaneously by a continuous IR analyser and by gas chromatography, and identical results were obtained. Additionally, we also performed some selected FTIR measurements and the FTIR CO determinations coincided with the CG and continuous analysers. Therefore, and in order to further prove if this early experimental CO formation is an experimental artifact or a phenomenon effectively occurring during  $\text{CH}_3\text{SH}$  conversion, we decided to do an additional experiment in a different experimental setup [18], which has been used with success in other studies addressing sulphur chemistry (e.g. [33]). This setup, which has significantly different dimensions compared to the one used in the rest of experiments, includes a flow tubular reactor where reactants enter premixed. The results of this experiment (experiment 8 in Table 1), together with model calculations, are shown in Figure 5. It can be observed that, despite the differences in the experimental conditions and installation used, the model can reproduce the experimental observations with the exception of the concentration of CO in the 800 to 1200 K temperature range, where the same early formation of CO is attained. Thus, from these results, we can conclude that the early formation of CO effectively occurs. However, we are not able to predict this early CO formation with the current knowledge of the chemistry addressing the conversion of  $\text{CH}_3\text{SH}$  and other thiols.



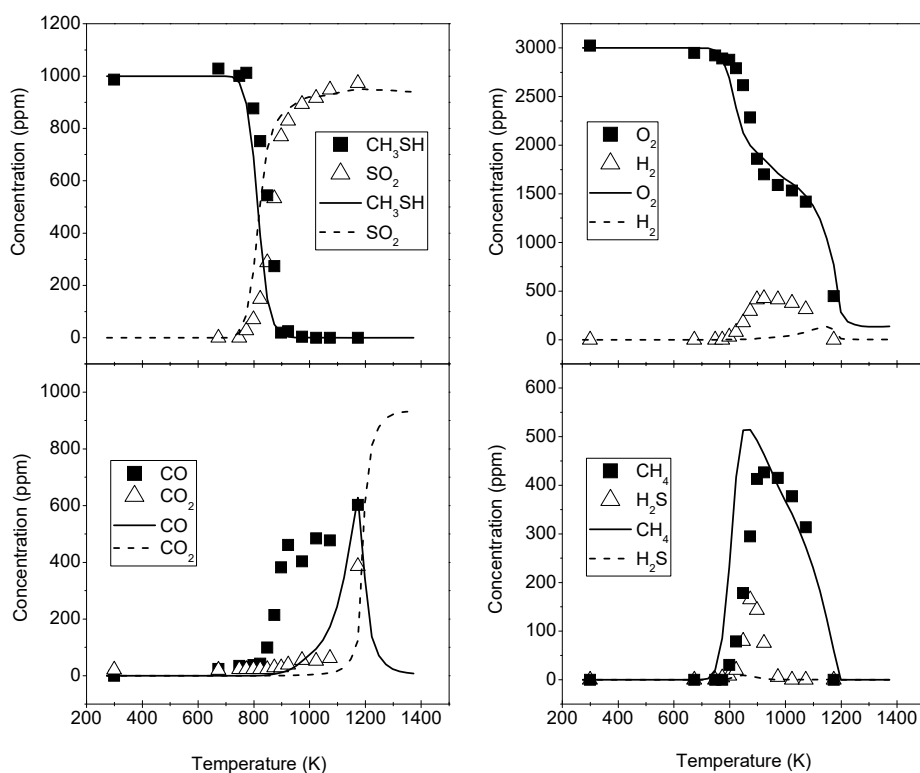
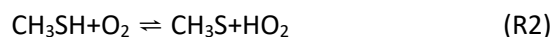
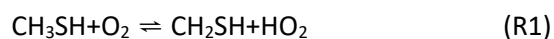


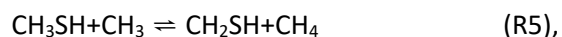
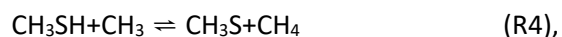
Figure 5. Experimental and simulated results of experiment 8 in Table 1.

Figure 6 includes a reaction pathway diagram of  $\text{CH}_3\text{SH}$  conversion. At the beginning of reaction,  $\text{CH}_3\text{SH}$  is mainly decomposed or consumed by reaction with  $\text{O}_2$  (R1 and R2), with a minor contribution of thermal decomposition (R3),

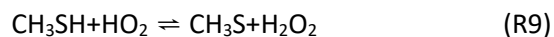
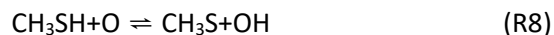
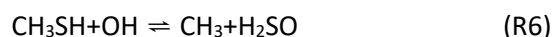


SH radicals contribute to S and  $\text{S}_2$  formation, which appear to be relevant for  $\text{CS}_2$  formation, as stated further below. A small fraction of SH radicals reacts with oxygen and follows the typical oxidation pathway for this species, as shown in Colom-Díaz et al. [33]. The SH radicals formed in reaction R3 also participate in a minority pathway, reacting with  $\text{C}_2\text{H}_4$ , which in turn is formed from ethane generated from  $\text{CH}_3$  recombination, leading to  $\text{CH}_2\text{CH}_2\text{SH}$ , which participates in an isomerization cycle to  $\text{CH}_3\text{CH}_2\text{S}$  and goes back to  $\text{CH}_2\text{CH}_2\text{SH}$ .

Apart from the  $\text{CH}_3\text{SH} + \text{O}_2$  reaction, as soon as methyl radicals are formed (e.g. reaction R3), they react with  $\text{CH}_3\text{SH}$  leading to the formation of two isomers,  $\text{CH}_3\text{S}$  and  $\text{CH}_2\text{SH}$ , (reactions R4 and R5):

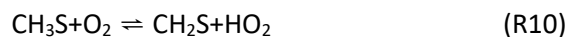


and once the O/H radical pool builds up, reactions with radicals also occur (R6-R9), with reaction (R6) as the dominant one:



The  $\text{CH}_3\text{SH}$  subset was taken entirely from the work of Van der Vijver et al. [24], which was developed for the thermal decomposition of diethyl sulphide and ethyl methyl sulphide using a rule based kinetic model generator Genesys, with certain modifications as discussed later, and from the works of Zheng et al. [7, 23] of their studies on ethyl methyl sulphide and diethyl sulphide oxidation. As seen, the mechanism describes properly methanethiol conversion and, thus, it can be considered as appropriate.

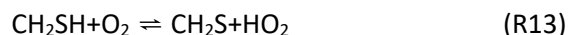
The methyl thiyl radical ( $\text{CH}_3\text{S}$ ), which is formed in considerable amounts mainly through reaction R4, basically reacts with  $\text{O}_2$ , independently of the stoichiometry. The  $\text{CH}_3\text{S} + \text{O}_2$  reaction has three product channels (R10-R12):



with the first two ones dominant under the conditions of the present work.

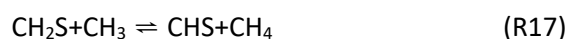
For this reaction ( $\text{CH}_3\text{S} + \text{O}_2 \rightarrow \text{products}$ ), there are only experimental room temperature upper-limit determinations [38, 39]. More recently, the reaction was studied by Zhu and Bozzelli [40], who analysed a number of possible reaction channels for this reaction relevant for atmospheric chemistry by means of DFT and ab initio methods, and isolated the dominant channels which appear to be those mentioned above. In the present work, the determinations of Zhu and Bozzelli [40] for this reaction rate have been adopted.

$\text{CH}_2\text{SH}$ , formed in reaction R1, is mainly converted into the  $\text{CH}_2\text{S}$  radical by reaction with oxygen,



for which the rate constant provided by Zheng et al. [23] has been used.

$\text{CH}_2\text{S}$  is an important intermediate, originated from both  $\text{CH}_3\text{S}$  and  $\text{CH}_2\text{SH}$  (reactions R10 and R13, respectively). Once formed,  $\text{CH}_2\text{S}$  reacts with the O/H radical pool and also with  $\text{CH}_3$  radicals, which are present in significant amounts for all the conditions studied, through reactions R14-R17, giving CHS.



$\text{CS}_2$  is formed through the reaction of CHs with S or  $\text{S}_2$ , formed from SO and SH, in reactions R18 and R19:



$\text{CS}_2$  is finally directly converted into  $\text{SO}_2$ . Compared to the  $\text{CH}_3\text{S} + \text{O}_2 \rightleftharpoons \text{CH}_3 + \text{SO}_2$  reaction path forming  $\text{SO}_2$ , the  $\text{CH}_3\text{SH} \rightarrow \text{CH}_2\text{SH}/\text{CH}_3\text{S} \rightarrow \text{CH}_2\text{S} \rightarrow \text{CHS} \rightarrow \text{CS}_2 \rightarrow \text{SO}_2$  sequence is more relevant as the stoichiometry becomes fuel richer, being dominant for the richest conditions studied in the present work.

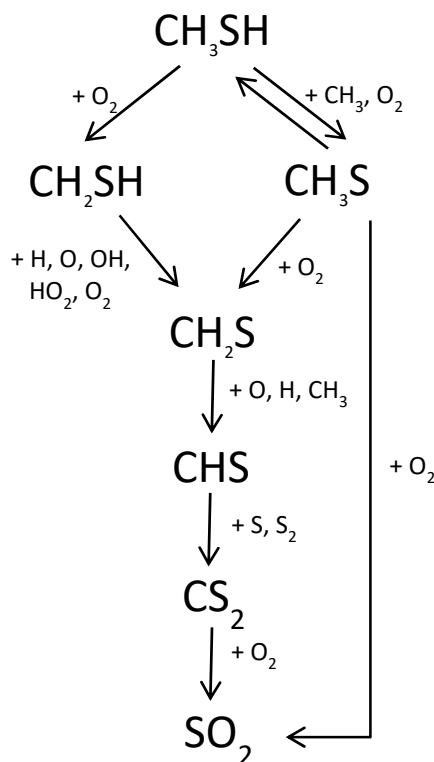


Figure 6. Main reaction pathway diagram of  $\text{CH}_3\text{SH}$  conversion to  $\text{SO}_2$ .

Figure 7 shows, as an example, the sensitivity analysis performed for  $\text{CH}_3\text{SH}$ , at  $\lambda=0.99$ , at the temperature of 798 K and at the outlet of the reaction zone. As seen, the results are mainly sensitive to the  $\text{CH}_3\text{SH} + \text{CH}_3$  reaction producing  $\text{CH}_2\text{SH}$ , which is an important conversion pathway for  $\text{CH}_3\text{SH}$  once conversion has been initiated, and the dominant one under rich conditions. Reactions of  $\text{CH}_3\text{SH} + \text{CH}_3$  have been taken from the mechanism of Gersen et al. [30] and were also included in the mechanism of Zheng et al. [23], used for the study of diethyl sulphide oxidation with success and to evaluate the pyrolysis and oxidation of sulphur mustard simulates [41]. The kinetic parameters of the  $\text{CH}_3\text{SH} + \text{CH}_3$  reaction are theoretical estimates. Therefore, since these reactions appear to show a significant sensitivity under the studied conditions of this work, a proper determination of them, not available at present, would be desirable. Also, reactions controlling the radical H/O and  $\text{CH}_3$  pool appear to exhibit a high sensitivity on the model calculations for both  $\text{CH}_3\text{SH}$  and CO, which are representative of the full oxidation process of methanethiol. Similar results, not shown, are obtained for other stoichiometries considered.

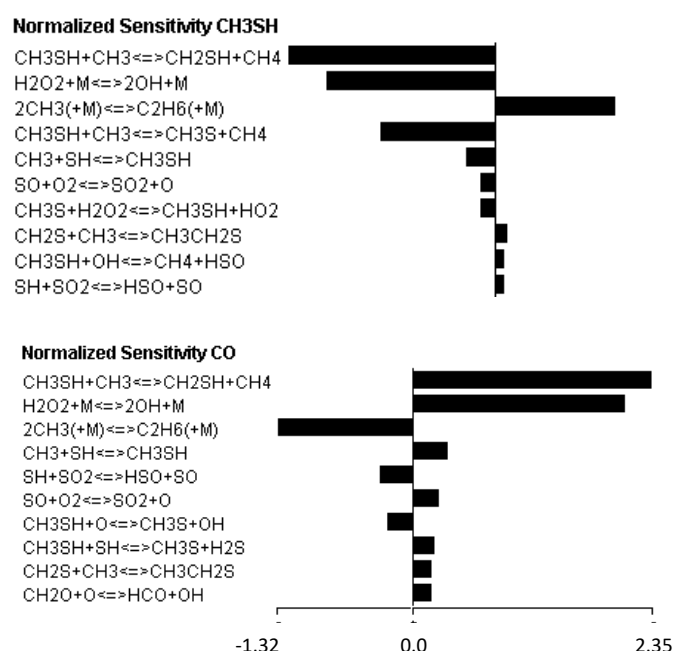


Figure 7. Normalized sensitivity analysis results for CH<sub>3</sub>SH and CO, for  $\lambda=0.99$  (set 4 in Table 1) at the outlet of the reaction zone at the temperature of 798 K.

## CONCLUSIONS

Oxidation of CH<sub>3</sub>SH at atmospheric pressure has been studied under different reaction atmospheres, varying the air excess ratio ( $\lambda$ ) from almost pyrolytic conditions ( $\lambda=0.01$ ) to oxidizing conditions ( $\lambda=5.08$ ). The experiments were carried out in a quartz tubular flow reactor, in the 300-1400 K temperature range and concentrations of CH<sub>3</sub>SH, H<sub>2</sub>S, SO<sub>2</sub>, COS, CS<sub>2</sub>, CH<sub>4</sub>, H<sub>2</sub>, O<sub>2</sub>, CO and CO<sub>2</sub> were determined. CH<sub>3</sub>SH conversion starts between 800 and 1000 K, shifting toward lower temperatures as  $\lambda$  is higher, and most of the conversion occurs in a narrow temperature window. The results obtained with and without water vapour are similar for all the species measured. The main products of CH<sub>3</sub>SH conversion appear to be H<sub>2</sub>, CO, CO<sub>2</sub> and SO<sub>2</sub>, with a remarkable formation of CS<sub>2</sub>, while COS only was detected under reducing conditions ( $\lambda<0.7$ ) and at the highest temperatures studied.

A detailed kinetic mechanism for the conversion of CH<sub>3</sub>SH under the present conditions has been compiled based on different literature reaction subsets, and has been used to simulate the experimental results obtained in the present work, with a general good agreement between experimental results and simulations. The exception is the failure in the mechanism to predict the experimentally early CO formation found, for all the conditions studied, and from experiments carried out in different experimental installations. Additionally, the mechanism has been used to identify the main reactions governing the conversion of CH<sub>3</sub>SH and the reactions to which the results are more sensitive.

## ACKNOWLEDGEMENT

The authors express their gratitude to Aragón Government and European Social Fund (GPT group), and to MINECO and FEDER (Project CTQ2015-65226) for financial support. The assistance of J.M. Colom-Díaz with the experimental setup 2 is highly acknowledged.

## REFERENCES

- [1] M. Bacanelli, S. Langé, M.V. Rocco, L.A. Pellegrini, E. Colombo. Low temperature techniques for natural gas purification and LNG production: An energy and exergy analysis, *Appl. Energy* 2016; 180: 546-59.
- [2] US Department of Energy. Report of Basic Research Needs for Clean and Efficient Combustion of 21<sup>st</sup> Century Transportation Fuels, 2016. <https://www.osti.gov/servlets/purl/935428-bbBji1/>, accessed 10/24/2018.
- [3] C. He, F. You. [Deciphering the true life cycle environmental impacts and costs of the mega-scale shale gas-to-olefins projects in the United States](#), *Energy Environ. Sci.* 2016; 9: 820-40.
- [4] R.K. Rahman, A. Raj. [A reaction kinetics study and model development to predict the formation and destruction of organosulfur species \(carbonyl sulfide and mercaptans\) in Claus furnace](#), *Int. J. Chem. Kin.* 2018; 50: 880-896.
- [5] C.M. Wong, R.W. Crawford, A.K. Burnham. Determination of sulfur-containing gases from oil shale pyrolysis by triple quadrupole mass spectrometry, *Anal. Chem.* 1984; 56: 390-395.
- [6] A. Slavens, J. Llamas, S. O'Dell, L. Francoviglia. Enhanced sulphur recovery from lean acid gases containing COS and mercaptans, Gas 2010 conference, 7-17, 2010. [www.digitalrefining.com/article/1000468](http://www.digitalrefining.com/article/1000468) (accessed the 10<sup>th</sup> January 2019).
- [7] X. Zheng, E.M. Fisher, F.C. Gouldin, W. Bozzelli. Pyrolysis and oxidation of ethyl methyl sulfide in a flow reactor. *Combust. Flame* 2011; 158: 1049-58.
- [8] Y. Yang, Q.H. Wang, X.F. Lu, J.B. Li and Z. Liu. Combustion behaviors and pollutant emission characteristics of low calorific oil shale and its semi-coke in a lab-scale fluidized bed combustor, *Appl. Energy* 2018; 211: 631-8.
- [9] P. Glarborg, P. Marshall. [Oxidation of Reduced Sulfur Species: Carbonyl Sulfide](#), *Int. J. Chem. Kinet.* 2013; 45: 429-439.
- [10] P. Glarborg, P. Marshall, J. Troe. Temperature and Pressure Dependence of the Reaction S plus CS ( plus M) -> CS<sub>2</sub> (+M), *J. Phys. Chem. A.* 2015; 119: 7277-7281.
- [11] V. Azatyan, U.M. Gershenson, E.N. Sakissyan, G.A. Sachyan, A.B. Nalbandyan. Investigation of low-pressure flames of a number of compounds containing sulfur by the ESR method, *Proc. Combust. Inst.* 1969; 12: 989-994.
- [12] J.E. Lovelock, R.J. Maggs, R.A. Rasmussen. Atmospheric dimethyl sulphide and the natural sulphur cycle, *Nature* 1972; 237, 452-3.
- [13] D. Grosjean. Photooxidation of methyl sulfide, ethyl sulfide, and methanethiol, *Env. Sci. Technol.* 1984; 18: 460-8.

- [14] M. Chen, X.Z. Yao, R.C. Ma, Q.C. Song, Y.Y. Long, R. He. Methanethiol generation potential from anaerobic degradation of municipal solid waste in landfills, *Env. Sci. Pollut. Res.* 2017; 24: 23992-4001.
- [15] L. Masgrau, À. González-Lafont, J.M. Lluch. Variational transition-state theory rate constant calculations of the OH+CH<sub>3</sub>SH reaction and several isotopic variants, *J. Phys. Chem.* 2003; 107: 4490-4496.
- [16] M.U. Alzueta, R. Bilbao, M. Finestra. Methanol oxidation and its interaction with nitric oxide, *Energy Fuels* 2001; 15: 724-9.
- [17] M.U. Alzueta, P. Glarborg, K. Dam-Johansen. Low temperature interactions between hydrocarbons and nitric oxide, *Combust. Flame* 1997; 109: 25-36.
- [18] L. Marrodán, A. Millera, R. Bilbao, M.U. Alzueta. High-pressure study of methyl formate oxidation and its interaction with NO, *Energy Fuels* 2014; 28: 6107-15.
- [19] M.U. Alzueta, R. Bilbao, P. Glarborg. Inhibition and sensitization of fuel oxidation by SO<sub>2</sub>, *Combust. Flame* 2001; 1127: 2234-51.
- [20] P. Glarborg, D. Kubel, K. Dam-Johansen, H.M. Chiang, J.W. Bozzelli. Impact of SO<sub>2</sub> and NO on CO oxidation under post-flame conditions, *Int. J. Chem. Kinet.* 1996; 28: 773-80.
- [21] P. Glarborg, M.U. Alzueta, K. Dam-Johansen, J.A. Miller. Kinetic modelling of hydrocarbon/nitric oxide interactions in a flow reactor, *Combust. Flame* 1998; 115: 1-27.
- [22] J. Giménez-López, M. Martínez, A. Millera, R. Bilbao, M.U. Alzueta. SO<sub>2</sub> effects on CO oxidation in a CO<sub>2</sub> atmosphere, characteristic of oxy-fuel conditions, *Combust. Flame* 2011; 158: 48-56.
- [23] X. Zheng, J.W. Bozzelli, E.M. Fisher, F.C. Gouldin, L. Zhu. Experimental and computational study of oxidation of diethyl sulfide in a flow reactor, *Proc. Combust. Inst.* 2011; 33: 467-75.
- [24] R. Van de Vijver, N.M. Vandewiele, A.G. Vandeputte, K.M. Van Geem, M.F. Reyniers, W.H. Green, G.B. Marin. Rule-based ad initio kinetic model for alkyl sulfide pyrolysis, *Chem. Eng. J.* 2015; 278: 385-93.
- [25] A.G. Vandeputte, M.F. Reyniers, G.B. Marin. A theoretical study of the thermodynamics and kinetics of small organosulfur compounds, *Theor. Chem. Acc.* 2009; 123: 391-412.
- [26] A.G. Vandeputte, M.F. Reyniers, G.B. Marin. Theoretical study of the thermal decomposition of dimethyl disulfide, *J. Phys. Chem.* 2010; 114: 10531-49.
- [27] A.G. Vandeputte, M.F. Reyniers, G.B. Marin. Kinetics of alpha hydrogen abstractions from thiols, sulfides and thiocarbonyl compounds, *Phys. Chem. Chem. Phys.* 2012; 14: 12773-93.
- [28] A.G. Vandeputte, M.F. Reyniers, G.B. Marin. Kinetics of homolytic substitutions by hydrogen atoms at thiols and sulfides, *Chem. Phys. Chem.* 2013; 14: 1703-22.
- [29] A.G. Vandeputte, M.F. Reyniers, G.B. Marin. Kinetic modeling of hydrogen abstractions involving sulfur radicals, *Chem. Phys. Chem.*, 2013; 14: 3751-71.
- [30] S. Gersen, M. Van Essen, H. Darneveil, H. Hashemi, C.T. Rasmussen. P. Glarborg, H. Levinsky. Experimental and modeling investigation of the effect of H<sub>2</sub>S addition to methane on the ignition and oxidation at high pressures, *Energy Fuels* 2017; 31: 2175-82.

- [31] M. Abián, M. Cebrián, A. Millera, R. Bilbao, M.U. Alzueta. Kinetic study of the moist CS<sub>2</sub> and COS under combustion conditions. Experiments and modelling, *Combust. Flame* 2015; 162: 2119-27.
- [32] M. Abián, A. Millera, R. Bilbao, M.U. Alzueta. Impact of SO<sub>2</sub> on the formation of soot from ethylene pyrolysis, *Fuel* 2015; 159: 550-8.
- [33] J.M. Colom-Díaz, M. Abián, M.Y. Ballester, A. Millera, R. Bilbao, M.U. Alzueta. H<sub>2</sub>S conversion in a tubular flow reactor. Experiments and kinetic modeling, *Proc. Combust. Inst.* 2019; 37 (in press), doi:10.1016/proci.2018.05.005.
- [34] K. Sendt, M. Jazbec, B.S. Haynes. Chemical kinetic modeling of the H/S system: H<sub>2</sub>S thermolysis and H<sub>2</sub> sulfidation, *Proc. Combust. Inst.* 2003; 29: 2439-46.
- [35] C.R. Zhou, K. Sendt, B.S. Haynes. Experimental and kinetic modeling study of H<sub>2</sub>S oxidation, *Proc. Combust. Inst.* 2013; 34: 625-632.
- [36] Y. Song, H. Hashemi, J.M. Christensen, C. Zou, B.S. Haynes, P. Marshall, P. Glarborg. An exploratory flow reactor study of H<sub>2</sub>S oxidation at 30-100 bar, *Int. J. Chem. Kin.* 2017; 49: 37-52.
- [37] CHEMKIN-PRO 15131. Reaction Design, 2013.
- [38] R.J. Balla, H.H. Nelson, J.R. McDonald. Kinetics of the reaction of CH<sub>3</sub>S with NO, NO<sub>2</sub> and O<sub>2</sub>, *Chem. Phys.* 1986; 109: 101-107.
- [39] G.S. Tyndall, A.R. Ravishankara. Kinetics of the reaction of CH<sub>3</sub>S with O<sub>3</sub> at 298 K, *J. Phys. Chem.* 1989; 93: 4707-10.
- [40] L. Zhu, J.W. Bozzelli. Kinetics of the multichannel reaction of methanethiyl radical (CH<sub>3</sub>S) with O<sub>2</sub>, *J. Phys. Chem.* 2006; 110: 6923-6937.
- [41] X. Zheng, 2011. Pyrolysis and oxidation of sulphur mustard simulants. PhD thesis, Cornell University.